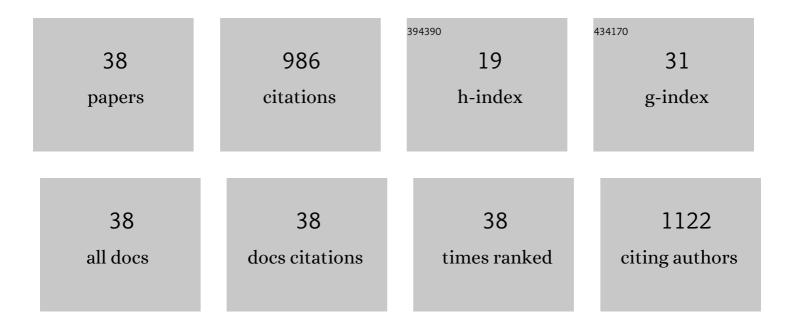
Jun Zhao

List of Publications by Year in descending order

Source: https://exaly.com/author-pdf/3755127/publications.pdf Version: 2024-02-01



#	Article	IF	CITATIONS
1	Machine Learning Based Longâ€Term Water Quality in the Turbid Pearl River Estuary, China. Journal of Geophysical Research: Oceans, 2022, 127, .	2.6	15
2	Estimation of vertical size-fractionated phytoplankton primary production in the northern South China Sea. Ecological Indicators, 2022, 135, 108546.	6.3	5
3	Mapping Diurnal Variability of the Wintertime Pearl River Plume Front from Himawari-8 Geostationary Satellite Observations. Water (Switzerland), 2022, 14, 43.	2.7	4
4	An Objective Method with a Continuity Constraint for Improving Surface Velocity Estimates from the Geostationary Ocean Color Imager. Remote Sensing, 2022, 14, 14.	4.0	2
5	Atmospheric Sulfuric Acid Dimer Formation in a Polluted Environment. International Journal of Environmental Research and Public Health, 2022, 19, 6848.	2.6	0
6	A novel technique for ship wake detection from optical images. Remote Sensing of Environment, 2021, 258, 112375.	11.0	25
7	Characterization of dicarboxylic acids, oxoacids, and α-dicarbonyls in PM2.5 within the urban boundary layer in southern China: Sources and formation pathways. Environmental Pollution, 2021, 285, 117185.	7.5	11
8	Assessing responses of phytoplankton to consecutive typhoons by combining Argo, remote sensing and numerical simulation data. Science of the Total Environment, 2021, 790, 148086.	8.0	12
9	Source apportionment of marine atmospheric aerosols in northern South China Sea during summertime 2018. Environmental Pollution, 2021, 289, 117948.	7.5	10
10	Two-Decade Variability of Sea Surface Temperature and Chlorophyll-a in the Northern South China Sea as Revealed by Reconstructed Cloud-Free Satellite Data. IEEE Transactions on Geoscience and Remote Sensing, 2021, 59, 9033-9046.	6.3	16
11	A Floating Optical Buoy (FOBY) for Direct Measurement of Waterâ€Leaving Radiance Based on the Skylightâ€Blocked Approach (SBA): An Experiment in Honghu Lake, China. Journal of Geophysical Research: Oceans, 2020, 125, e2020JC016322.	2.6	3
12	Assessing the Effects of the Hong Kongâ€Zhuhaiâ€Macau Bridge on the Total Suspended Solids in the Pearl River Estuary Based on Landsat Time Series. Journal of Geophysical Research: Oceans, 2020, 125, e2020JC016202.	2.6	14
13	In search of floating algae and other organisms in global oceans and lakes. Remote Sensing of Environment, 2020, 239, 111659.	11.0	52
14	Simulation of Kelvin wakes in optical images of rough sea surface. Applied Ocean Research, 2019, 89, 36-43.	4.1	11
15	Estimation of suspended particulate matter in turbid coastal waters: application to hyperspectral satellite imagery. Optics Express, 2018, 26, 10476.	3.4	14
16	Estimating CDOM Concentration in Highly Turbid Estuarine Coastal Waters. Journal of Geophysical Research: Oceans, 2018, 123, 5856-5873.	2.6	22
17	Remotely sensed sea surface salinity in the hyper-saline Arabian Gulf: Application to landsat 8 OLI data. Estuarine, Coastal and Shelf Science, 2017, 187, 168-177.	2.1	29
18	Analysis of bloom conditions in fall 2013 in the Strait of Hormuz using satellite observations and model simulations. Marine Pollution Bulletin, 2017, 115, 315-323.	5.0	2

Jun Zhao

#	Article	IF	CITATIONS
19	Improved atmospheric correction and chlorophyll-a remote sensing models for turbid waters in a dusty environment. ISPRS Journal of Photogrammetry and Remote Sensing, 2017, 133, 46-60.	11.1	23
20	A MODIS-Based Robust Satellite Technique (RST) for Timely Detection of Oil Spilled Areas. Remote Sensing, 2017, 9, 128.	4.0	23
21	MODIS-Based Mapping of Secchi Disk Depth Using a Qualitative Algorithm in the Shallow Arabian Gulf. Remote Sensing, 2016, 8, 423.	4.0	21
22	Monitoring HABs in the shallow Arabian Gulf using a qualitative satellite-based index. International Journal of Remote Sensing, 2016, 37, 1937-1954.	2.9	16
23	A semianalytical algorithm for quantitatively estimating sediment and atmospheric deposition flux from MODISâ€derived sea ice albedo in the Bohai Sea, China. Journal of Geophysical Research: Oceans, 2016, 121, 3450-3464.	2.6	1
24	Modeling of circulation in the <scp>A</scp> rabian <scp>G</scp> ulf and the <scp>S</scp> ea of <scp>O</scp> man: Skill assessment and seasonal thermohaline structure. Journal of Geophysical Research: Oceans, 2016, 121, 1700-1720.	2.6	56
25	Analysis of the spatio-temporal variability of seawater quality in the southeastern Arabian Gulf. Marine Pollution Bulletin, 2016, 106, 127-138.	5.0	21
26	Characterization of harmful algal blooms (HABs) in the Arabian Gulf and the Sea of Oman using MERIS fluorescence data. ISPRS Journal of Photogrammetry and Remote Sensing, 2015, 101, 125-136.	11.1	49
27	Satellite-Based Tracking of Oil Pollution in the Arabian Gulf and the Sea of Oman. Canadian Journal of Remote Sensing, 2015, 41, 113-125.	2.4	35
28	Remote sensing of red tide in the Arabian Gulf. , 2014, , .		0
29	Exploring the potential of optical remote sensing for oil spill detection in shallow coastal waters-a case study in the Arabian Gulf. Optics Express, 2014, 22, 13755.	3.4	86
30	Monitoring red tide with satellite imagery and numerical models: A case study in the Arabian Gulf. Marine Pollution Bulletin, 2014, 79, 305-313.	5.0	78
31	Assessment of satellite-derived diffuse attenuation coefficients and euphotic depths in south Florida coastal waters. Remote Sensing of Environment, 2013, 131, 38-50.	11.0	62
32	Three-dimensional structure of a Karenia brevis bloom: Observations from gliders, satellites, and field measurements. Harmful Algae, 2013, 29, 22-30.	4.8	25
33	Satellite-Observed Black Water Events off Southwest Florida: Implications for Coral Reef Health in the Florida Keys National Marine Sanctuary. Remote Sensing, 2013, 5, 415-431.	4.0	26
34	First attempt to derive chlorophyll-ausing natural fluorescence in Northern South China Sea. Remote Sensing Letters, 2012, 3, 249-258.	1.4	5
35	Did the northeastern Gulf of Mexico become greener after the Deepwater Horizon oil spill?. Geophysical Research Letters, 2011, 38, .	4.0	117
36	Variation of particulate organic carbon and its relationship with bio-optical properties during a phytoplankton bloom in the Pearl River estuary. Marine Pollution Bulletin, 2011, 62, 1939-1947.	5.0	31

#	Article	IF	CITATIONS
37	The variations in optical properties of CDOM throughout an algal bloom event. Estuarine, Coastal and Shelf Science, 2009, 82, 225-232.	2.1	41
38	Measuring natural phytoplankton fluorescence and biomass: A case study of algal bloom in the Pearl River estuary. Marine Pollution Bulletin, 2008, 56, 1795-1801.	5.0	23